BEHAVIOR OF FATIGUE CRACK EXTENSION IN MICROELECTRONICS SOLDER JOINTS

MAKIO IINO and KEN KAMINISHI
Department of Mechanical Engineering, Yamaguchi University

For fatigue life prediction of solder joints of an electronic package experimental and numerical analyses were performed. The experiments consisted of displacement-controlled fatigue tests on a solder joint of a surface-mounted electronic package model at different temperatures, cycling frequencies and controlled displacement amplitudes, the joint material being composed of 53% Sn - 45% Pb - 2% Bi. The numerical analyses consisted of FEM analyses for two-dimensional elasto-inelastic stress distribution at and around crack tip, prediction of crack extension path and estimation of fatigue life. FEM analysis results are in general satisfactory agreement with experimental observations including fatigue crack extension path. The analysis disclosed that crack extension per cycle is controlled by a maximum opening stress range at crack tip in plastic zone under rather complicated stress tensor fields. Further, expressing the fatigue crack extension rate in terms of applied displacement amplitude and crack length a relationship between the crack length and the number of cycles was attained, which determines fatigue crack initiation and propagation lives.

Keywords *: Microelectronics solder joint, Surface-mounted electronic package model, Elasto-inelastic stress analysis, Fatigue crack extension path, Fatigue life*

1. INTRODUCTION

For the build-up of basic reliability data of solder joints in electronic systems, unavoidably exposed to mechanical and/or thermal fatigue conditions, there have been not a few works from several aspects discussing degradation of solder joint materials induced by mechanical straining under repeated loadings[1], or equivalent creep-induced damage concept[2][3]. Shiratori[3] proposed that a thermal fatigue test may equivalently be replaced by a mechanical cycle test, based upon numerical analytical prediction and experimental verification; they observed an approximate equivalence of cycles-to-failure to inelastic equivalent strain range relation in a comparatively low strain rate region of $2.0 \cdot 10^{-5}$ to $4.0 \cdot 10^{-3} s^{-1}$, the temperatures for thermal fatigue test and mechanical cycle test being in a range of -20 to 150℃and isothermal 20℃, respectively, where cycles-to-failure signifies number of cycles to fatigue crack initiation.

Taneda et al[4] conducted torsion fatigue tests on 60Sn-40Pb, and a low melting-point 37Sn-45Pb-18Bi, solders at 303K under different cyclic frequencies, and experimentally determined parameters appearing in a fatigue life-frequency-plastic strain range relationship proposed by Coffin[5]. By applying the strain range partitioning approarch, with linear cumulative damage concept, and using material-dependent parameters, Taneda et al[4][6] proposed a fatigue life prediction formula, expressing number of cycles to failure as a function of cyclic frequency and equivalent inelastic strain range, which can be understood to successfuly incorporate a creep damage effect.

It seems, however, that works conducted up to date concerning reliability of the electronic solder joints have been confined to discussions of fatigue crack initiation lives; there have actually been very little works treating the problem of a fatigue crack extension process, which is experimentally pointed out to occupy an important part of the total life of the microelectronics solder joints[4]. Under the above-mentioned background the purpose of the present work is to investigate crack extension behavior in a product size model of QFP(a quad flat package) by isothermally conducted mechanical cycle tests at 303K and 318K under cyclic frequencies of 0.1 and 1.0 Hz.

2. TESTING PROCEDURES

The top surface of the test model is adhered to a bar, which is in turn clamped to a displacement-controlled reciprocating spindle, as shown in Figure

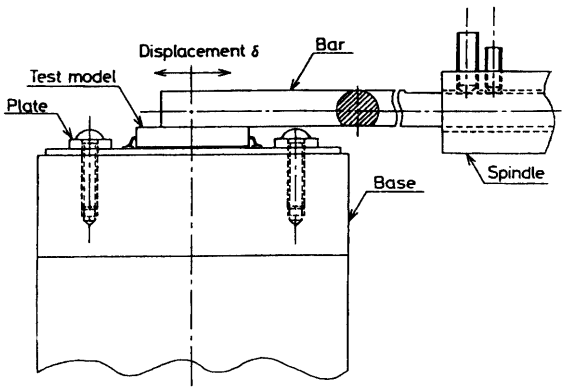

Fig. 1 Fitting of test model to fatigue testing system
Test model consists of a quad flat package, lead wire, substrate and solder joint.

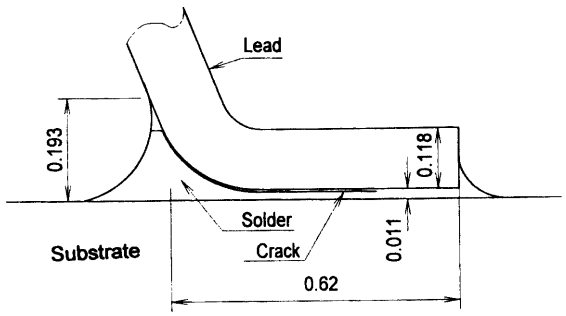

Fig. 2 Geometry of lead wire and solder joint with an illustration of crack path

1. Motion of the spindle, and the rod, can be controlled to reciprocating displacement of $\pm 30\,\mu$ m or $\pm 60\,\mu$ m by combined use of a variable speed motor and a cam.

A solder joint and lead wire with the test substrate is shown magnified in Figure 2. Thickness of lead wire, 0.118 mm, and fillet hight, 0.193 mm, indicated in the figure are averages of several measured values. Chemical compositions and mechanical properties of the solder material used are given in Table 1. The substrate is made of glass epoxy resin, and the lead wire of 42 Alloy. The test is carried out at temperatures controlled to 303 $\pm$2K and 318 $\pm$2K, the reciprocating frequencies 0.1 and 1.0Hz and the displacement amplitudes being 30 and 60 μ m, the adopted combinations of which are listed in Table 2.

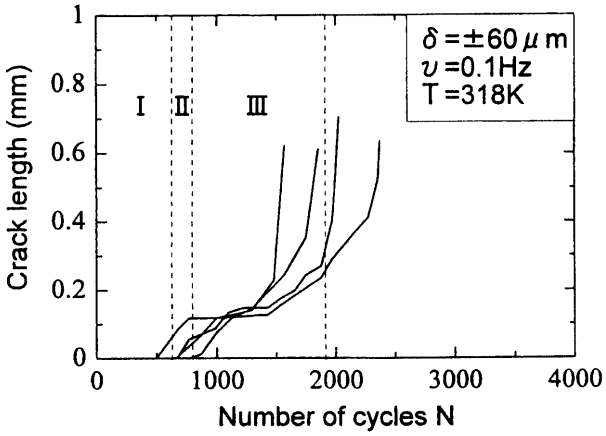

Fig. 3 Experimental plot of crack length against number of cycles

3. EXPERIMENTAL RESULTS

Typical plots of crack length versus number of cycles are presented in Figure 3. As shown in the figure, fatigue crack initiation or begining of visible crack growth takes place at several hundred cycles under indicated test conditions, and initial stage of crack growth starts rather discontinuously. Crack growth rate is rather abruptly reduced as crack length exceeds a critical value, a_c, which is approximately 0.1 mm, and after a plateau region or gradual rise, enters a region of accelerated increase, as crack length exceeds approximately 0.2 mm, until final unstability.

It is to be noted that the value of a_c accords with that at which crack arrives at the interface with lead wire, and the inception of rapid crack growth, 0.2 mm, is a distance around which a straight linear growth of crack becomes possible. Briefly, it would be reasonable to divide life to final failure into the three domains indicated in Figure 3, namely life to crack initiation(I), period from crack initiation to crack growth up to the interface with lead wire(II) and period for crack propagation along the solder-lead interface to final failure(III).

As for the influences of applied displacement amplitude, test temperature and test frequency upon fatigue life, it should be noted that that an increase in an applied amplitude from 30 μ m to 60 μ m reduced lives of domains II and III to a quarter respectively, while change in temperature, from 303 to 318K, and frequency, from 0.1 to 1.0Hz caused little change in fatigue life.

4. DISCUSSIONS

(1) Fracture criterion to predict crack extension path

In detrmining a crack extension path, preliminary considerations will be put forth below upon farcture criteria to predict the direction of crack extension. Such discussions will include the criteria of maximum tangential stress(MTS)[7], maximum energy-release rate(ERR)[8], minimum strain energy density(SED)[9] and modified SED[10][11]. In determining the reqired direction of crack extension, the former three criteria define an angle in a circle around the crack tip, at which a quantity in question is maximized for the angle to give the expected direction of crack extension. Sih [9] discussed the significance of the circle and considered that the radius, constrained to be a constant, must be greater than the radius of a core region defined by the limit of continuum mechanics. Among the proposals referred to above, however, the modified SED criterion may deserve the greatest attention for the reason to be described below. Theocaris[10], who proposed the modified SED criterion, considers that there is no need to put a circle around crack tip, and replaces the circular domain by a plastic zone developed around the crack tip prior to the onset of crack extension, and adopts for convenience the Mises criterion to define the elastic-plastic boundary. He thus describes the elastic-plastic boundary locus, $r = r(\theta)$, by the Mises yield condition expressed in terms of the distortional component, u_D, of elastic strain energy density, that is for plane stress

$$u_D = [(1+\nu)/3E][\sigma_1^2 + \sigma_2^2 - \sigma_1\sigma_2)] = u_{DO}, \quad (1)$$

along which a maximum is sought in the dilatational component, u_V, of elastic strain energy density,

$$u_V = [(1-2\nu)/6E][\sigma_1 + \sigma_2]^2, \quad (2)$$

thus assuring a maximization of the total elastic strain energy density there, which is assumed to define the direction of crack extension. In equations (1) and (2) σ_1 and σ_2 are the principal stresses, E and ν being Young's modulus and Posson's ratio, respectively. u_{DO} is a critical value of u_D, which can be expressed by $\sigma_Y^2/6\mu$ with σ_Y and μ being the unixial tensile yield strength and the shear modulus of the material, respectively. From equations(1) and (2) it is found that

$$u_V = [(1-2\nu)/2(1+\nu)]u_D + [(1-2\nu)/2E]\sigma_1\sigma_2. \quad (3)$$

Then along the yield locus $\partial u_V/\partial\theta$ is given by

$$\partial u_V/\partial\theta = [(1-2\nu)/2E]\partial[\sigma_1\sigma_2]/\partial\theta. \quad (4)$$

A maximum of u_V along the yield locus can be found by letting $\partial u_V/\partial\theta = 0$ in equation(4), i.e.,

$$\sigma_1\partial\sigma_2/\partial\theta + \sigma_2\partial\sigma_1/\partial\theta = 0. \quad (5)$$

Based upon the above reasonings and rejecting trivial cases, Theocaris[11] is lead to the condition,

$$\partial\sigma_2/\partial\theta = \partial\sigma_1/\partial\theta = 0, \quad (6)$$

which implies that the the maximum tangential principle stress(MTPS) criterion is an alternative expression of the modified SED criterion. The path for the maximization to be executed might not be confined to the yield locus, as proposed by Theocaris[10], but to the authors' mind may be generalized to that of a constant u_{DO}, e.g., the heavily deformed zone locus within the plastic zone.

In respect of the maximum tangential stress(MTS) criterion it can be said that this coincides with MTPS criterion sufficiently near the crack tip where the first term representation of stresses is accurate, although the coincidence depends on the adopted work-hardening model. Indeed, for a power-law hardening material[12], to which an Airy stress function, ϕ, of the form

$$\phi = [(1+n)^2/(2+n)]r^{(2+n)/(1+n)}f(\theta) \quad (7)$$

is introduced, near tip stresses are given by

$$\sigma_\theta = \partial^2\phi/\partial r^2 = r^{-n/(1+n)}f(\theta), \quad (8)$$

$$\tau_{r\theta} = -(\partial/\partial r)[(1/r)(\partial\phi/\partial\theta)]$$

$$= -[(1+n)/(2+n)]r^{-n/(1+n)}f'(\theta), \quad (9)$$

$$\sigma_r = (1/r)(\partial\phi/\partial r) + (1/r^2)(\partial^2\phi/\partial\theta^2)$$

$$= (1+n)r^{-n/(1+n)}[f(\theta) + \{(1+n)/(2+n)\}f''(\theta)], \quad (10)$$

where n is the work-hardening exponent, having a value of $0 \leqq n \leqq 1$. It follows that

$$\partial\sigma_\theta/\partial\theta = -[(2+n)/(1+n)]\tau_{r\theta}, \quad (11)$$

thus at a critical angle, $\theta = \theta_C$, of crack extension it should be valid that

$$\partial\sigma_\theta/\partial\theta = \tau_{r\theta} = 0, \quad (12)$$

which implies equivalence of MTS and MTPS criteria sufficiently near the crack tip. Following the above discussions a MTS criterion will be applied to

the determination of a critical angle, at a small radial distance, of crack extension in the following section

(2) Crack propagation life

Fatigue Crack Extension Analyses by FEM

The FEM program for crack extension analyses in this work is characterized by its capability of auto-

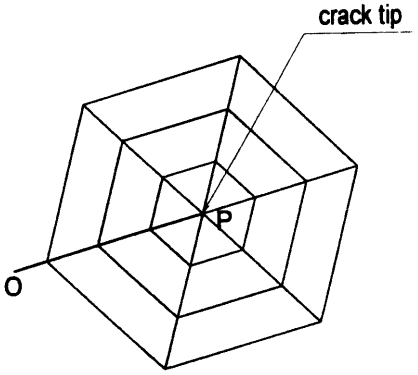

Fig. 4 Hexagonal super-element embedded in the near crack-tip region

OP indicates a crack having proceeded, with current crack tip being denoted by P, at which crack can shift its azimuth in the direction of MTS range.

matic re-allocation of elements around tip of an extending crack. It consitsts of programs for the automatic element re-generation, the element configuration in the near-tip region being provided by a special hexagonal super-element demonstrated in Figure 4, FEM for two-dimensional elasto-inelastic stress analyses, prediction of crack extension path and calculation of fatigue life. In Figure 4 OP indicates a crack having proceeded from the left, with a current crack tip being denoted by P, at which crack can shift its azimuth in accordance with the adopted fracture criterion to be discussed below.

In the process of crack extension it is found that general yielding proceeds in solder fillets. Here the linear fracture mechanics representation would be inappropriate to describe stress fields at crack tip to determine crack extension path. It is assumed in this instance that crack extends in the direction of maximum $\Delta\sigma_\theta$ at a small radial distance of r = d, where d is chosen to be a grain diameter's distance, 3.5 μ m, in solder materal. The maximum $\Delta\sigma_\theta$ at r = d is denoted by $(\Delta\sigma_\theta)_{CT}$ in Figure 5, where an example of plot of $(\Delta\sigma_\theta)_{CT}$ versus crack length is presented. It is characteristic of this plot that $(\Delta\sigma_\theta)_{CT}$, after an initial rise, rapidly decreases as the crack approaches a length of about 0.1 mm, followed by a gradual rise and a final rapid increase, as crack length exceeds 0.2 mm as shown in the figure.

In Figure 6 crack extension rate, da/dN, is plotted against the $(\Delta\sigma_\theta)_{CT}$, which describes crack extension rate as a function of $(\Delta\sigma_\theta)_{CT}$ of the form

$$da/dN = \beta\,[(\Delta\sigma_\theta)_{CT}]^{\alpha}, \qquad (13)$$

where numerical analysis showed that exponent α and factor β takes a constant value of

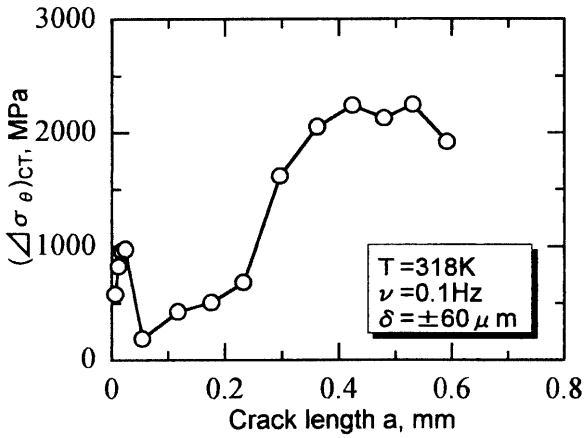

Fig. 5 Plot of computed maximum tangential stress range against observed crack length

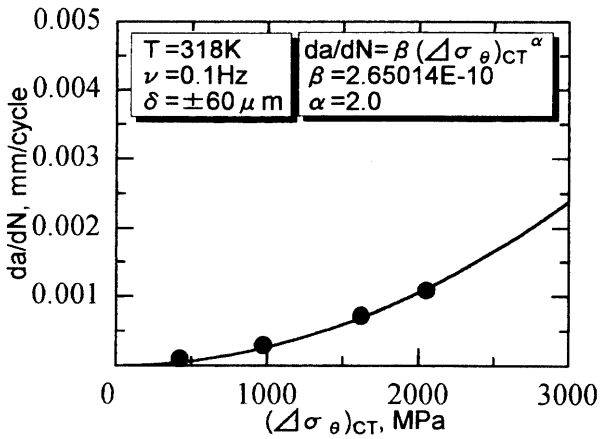

Fig. 6 Plot of experimentally determined crack growth rate against MTS range

$$\alpha = 2.0, \text{ and } \beta = 2.6\times10^{-10}\ \text{mm}^5/\text{N}^2, \qquad (14)$$

independently of test conditions, which encourages prediction of fatigue crack propagation life by integrating equation(13). It may be natural to assume that factor β depends on both material and test environment; the exponent α, however, is assumed to be independent of material, environment and mechanical test conditions.

Fatigue Crack Extension in Domain III

Domain III in Figure 3 plays an important role in the determination of a fatigue crack propagation life. So, that will be evaluated below. With the value of α given in equation(14) it is assumed that crack extension rate can be expressed by

$$da/dN = \gamma [\delta (\pi a)^{1/2}]^2, \qquad (15)$$

with γ being a factor which depends on solder material and strength of the solder-lead interface. In a small scale yielding model the quantity $[\delta (\pi a)^{1/2}]^2$ would be proportional to a crack tip opening displacement amplitude, which is directly proportional to the crack extension rate. It must be acknowledged, however, that the condition at and around the tip of a crack extending in solder material at ambient temperature or higher is not that of small scale yielding, but a specialized condition in that plastic zone produced at crack tip is geometrically forced to lie within the narrow path between the interface with the upper lead wire and the lower substrate illustrated in Figure 2.

Integration of equation(15) with respect to N renders crack length, a, as a function of number of cyclys, N, as

$$a = a_o + C\, e^{B(N - No)}, \qquad (16)$$

where B is a factor related to δ by $B = \pi \gamma \delta^2$ and C an integration constant. N_o and a_o in equation(16) denote initial values in domain III respectively. Figure 7 reproduces the experimental curve already shown in Figure 3, in which superimposed are the life-prediction formula given by equation(16), with γ, N_o and a_o being fitted to experiments. The factor γ was found to be independent of test conditions, which supports the previously stated assumption that γ depends on characteristics of solder material and strength of the solder-lead interface. Strong γ - dependence of crack length, a, expressed by equation(16) suggests that fatigue life of the sloder joint will be greatly influenced by a scatter in γ.

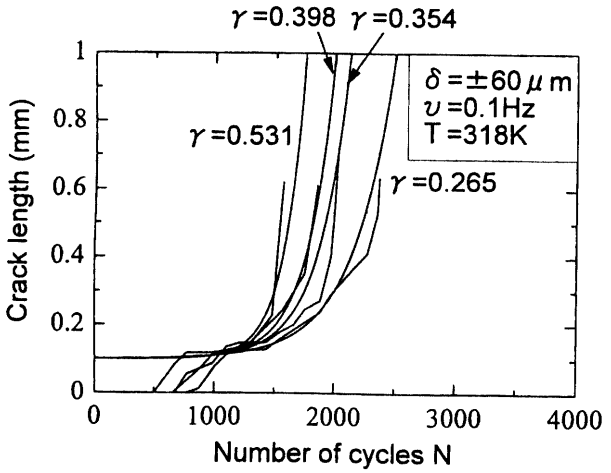

Fig.7 Relationship between crack length and number of cycles

CONCLUSIONS

For fatigue life prediction of solder joints of an electronic package experimetal and numerical analyses by FEM were performed. Experimentally obtained crack extension rate is found to be related to a maximum tangential stress range, $\Delta \sigma_{\theta max}$, at crack tip in FEM analysis by

$$da/dN = \beta [\Delta \sigma_{\theta max}]^{\alpha},$$

where $\alpha = 2.0$ and $\beta = 2.6 \cdot 10^{-10}$ mm^5/N^2 are determined independently of the test conditions. The FEM analysis result is in agreement with experimentally observed fatigue crack extension path. Further, expressing the fatigue crack extension rate in terms of applied displacement amplitude and crack length a relationship between the crack length and the number of cycle was attained, which determines fatigue crack initiation and propagation lives.

REFERENCES

1) Solomon, H.D., "High and Low Temperature Strain-Life Behavior of a Pb Rich Solder", ASME Journal of Electronics Packaging, Vol.112, 1990, pp.123-128.

2) Taneda, M and Kaminishi, K., "Effect of Cycling Frequency on Fatigue Life of Solder",Proceedings of the 1992 Joint ASME/JSME Conference on Electronic Packaging, ADVANCES IN ELECTRONIC PACKAGING, 1992, Vol.1, pp.337-342.

3) Shiratori, M and Qiang, Yu, "Fatigue-Strength Prediction of Microelectronics Solder Joints under Thermal Cyclic Loading", Proceedings of Inter Society Conference on THERMAL PHENOMENA IN ELECTRONIC SYSTEMS, May 29-June 1, 1996, Orlando, FL, USA, pp.151-157.

4) Taneda, M., Kaminishi, K., and Oku, Y., A Method for Fatigue Life Evaluation of Soler for Electronic Equipments, J. Mat. Sci., Vol.41. No.466, July 1992, pp.1047-1053.

5) Coffin, L.F., Proc. 2nd Int. Conf. Fracture, 1969, p.643

6) Taneda, M. and Motohiro, S., Fatigue Life of Solder under High Temperature, Technology Reports of the Fuculty of Engineering of Kyushu Kyoritsu University, No.18, March 1994, pp.27-36.

7) Erdogan, F. and Sih, G.C., On the Crack Extension in Plates under Plant Loading and Transverse Shear, J. Basic Egng., Trans. ASME, Vol. 88, Ser. D., 1963, pp.519-527.
8) Palaniswamy, K. and Knauss, E.G., Propagation of a Crack under General In-Plane Tension, Int. J. Fract. Mech., Vol. 8, 1972, pp.114-117.
9) Sih, G.C., Some Basic Problems In Fracture Mechanics and New Concepts, Engng. Fract. Mech., Vol. 5, 1973, pp.365-377.
10) Theocaris, P.S. and Adrianopoulos, N.P., Engng. Fract. Mech, Vol. 16, 1982, pp.425-432.
11) Theocaris, P.S, Affinity between Criteria Based on Components of Stresses or Strains and Energy Density, Int. J. Fract., Vol. 32, 1987, R51-R57.
12) Rice, J.R. and Rosengren, G.F., Plane Strain Deformation near a Crack Tip in a Power-Law Hardening Material, J. Mech. Phys. Solids, Vol. 16, 1968, pp.1-12.

(Received April 15, 1997)

Table 1 Chemical compositions and mechanical properties of solder materials tested

(a) Chemical compositions (wt pct)

Code	Sn	Pb	Bi	Sb	Cu	As
SPB	52.93	45.13	1.93	0.004	0.002	0.002

(b) Mechanical properties at 303 K

Shear strain rate(1/s)	Shear proof stress(Mpa)	Shear strength(MPa)	Shear modulus(MPa)
$6.73 \cdot 10^{-2}$	13.0	16.3	9.1
$2.05 \cdot 10^{-1}$	14.7	19.4	10.3
$7.01 \cdot 10^{-1}$	15.9	21.3	12.2
6.77	19.0	26.0	11.9

Table 2 Results of experiments and numerical analyses

Code	T (K)	ν (Hz)	δ (μm)	Nc	ε^{P}_{eq}(pct)	$[Nc]_{cal}$	$[Nc]_{cal}$ / Nc
1	318	1.0	±30	3287	0.5135	223	0.07
2	318	1.0	±60	337	1.3705	36	0.11
3	318	0.1	±30	1511	0.5469	292	0.19
4	318	0.1	±60	648	1.4149	60	0.09
5	303	0.1	±60	468	1.3299	42	0.09

マイクロエレクトロニクスはんだ接続部における疲労亀裂進展挙

飯野牧夫、上西　研

本報告は、LSIパッケージはんだ接続部の疲労寿命予測のために行った実験および数値解析に関するものである。実験には、表面実装型LSIパッケージサンプルを用い、変位制御型の疲労試験を種々の温度および繰り返し速度の下で実施した。はんだ材料の化学成分は53%Sn-45%Pb-2%Biである。数値解析は、疲労亀裂まわりの弾塑性応力のFEM解析、亀裂進展経路の予測および疲労寿命の評価からなる。解析結果は、実験結果とよく一致し、疲労亀裂の進展速度および方向は、複雑な塑性域応力場にある亀裂先端の周応力幅によって決定されることが示された。